JOURNAL OF APPLIED ELECTROCHEMISTRY 8 (1978) 479–482

SHORT COMMUNICATION

Orthogonal components of the impedance of batteries by a simple technique

S. SATHYANARAYANA, S. VENUGOPALAN*, M. L. GOPIKANTH

Department of Inorganic and Physical Chemistry, Indian Institute of Science, Bangalore 560 012, India

Received 6 February 1978

1. Introduction

Electrochemical power sources possess an internal impedance whose resistive and reactive (i.e., orthogonal) components are intimately related to the effective area of the electrodes, kinetics of the electrode processes and transport properties of the ions in the system. Interpretation of the impedance of batteries may therefore be expected to throw light on their performance characteristics as well as to assist quality control in production operations.

a.c. bridge methods have been described in the literature [1] to measure the resistance and capacitance components of the impedance of batteries. Although bridge measurements possess the well-known advantages due to a null method, applicability to measurement of battery impedance is often restricted because of the difficulty of having the required resistance and capacitance standards in a series configuration of the balancing arm; while the battery terminals acting as a d.c. power source lead to the difficulties of the balancing arm in a parallel configuration.

This paper describes a simple method of obtaining the equivalent series (or parallel) resistance and reactance components of the internal impedance of batteries and other electrochemical systems by a direct measurement of the phase-angle and modulus of the impedance with a vector lock-in amplifier. A somewhat similar method has been reported in [2]† and also in a recent work [3] to study the effective area of a porous metal–solution interface.

2. Principle of the method

As a circuit element a battery may always be represented as an ideal d.c. voltage source without any internal impedance, which is in series with a combination of a reactance (usually capacitive) and a resistance in either a parallel mode (R_p–C_p) or a series mode (R_s–C_s) as in Fig. 1.

As follows from circuit theory, the impedance vector $\mathbf{Z}$ is given as

$$\mathbf{Z} = R_s + \frac{1}{j\omega C_s} = \frac{1}{1/R_p + j\omega C_p} \qquad (1)$$

where $j = \sqrt{-1}$, $\omega = 2\pi f$ and f is the frequency in Hz.

The phase angle ϕ between the alternating current through the battery and alternating voltage across the battery is given as

$$\cot\phi = -\omega C_s R_s = -\frac{1}{\omega C_p R_p}. \qquad (2)$$

It follows from Equations 1 and 2 that

$$R_s = Z\cos\phi \qquad (3)$$

$$1/(\omega C_s) = Z\sin\phi \qquad (4)$$

$$R_p = Z/\cos\phi \qquad (5)$$

$$1/(\omega C_p) = Z/\sin\phi \qquad (6)$$

where Z is the modulus of $\mathbf{Z}$.

A measurement of Z and ϕ will therefore provide the components of the equivalent series circuit (Equations 3 and 4) and of the equivalent parallel circuit (Equations 5 and 6). Since the energy conversion processes in a battery are likely

* On leave from Tamil Nadu Alkaline Batteries Ltd, Madras, India.

† The method adopted in [2], however, introduces an unknown phase shift in the reference input caused by the reactance of the electrochemical system. This affects the measured phase angle to an uncertain extent.

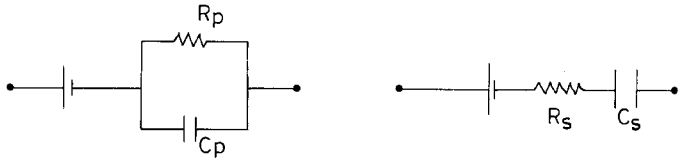

Fig. 1. Equivalent circuits of a battery as a circuit element.

to be related to one of the equivalent circuits in a simpler way than to the other, it is helpful to obtain both sets of desired data in a fairly direct manner, as by this method.

3. Experimental

The set-up shown in Fig. 2 was employed to measure Z and ϕ with ease.

The test battery B was excited with a sinusoidal voltage of about 10 mV amplitude across its terminals using a signal generator S. Isolation of the signal generator from the test circuit was achieved with a suitable transformer. The blocking capacitor C prevented the discharge of the battery in the otherwise low impedance circuit. The alternating current through the battery was obtained by measuring the voltage across R_1 with a digital voltmeter D of high input impedance. The alternating voltage across R_2 was used as the reference signal for the lock-in amplifier. The amplitude and phase of the alternating voltage across the battery was then measured by using this as the input signal to the lock-in amplifier. Since R_2 is a non-reactive resistor, the phase difference obtained is that between the voltage across the battery and the current through the battery together with the 180° phase shift caused by the grounding of the junction between B and R_2.

The measurements were carried out over a wide frequency range. The reproducibility of the impedance and phase measurements was usually better than 1%. The data were used to calculate R_s, C_s, R_p, and C_p using Equations 3–6.

In order to compare the results, the values of R_p and C_p were also measured with an impedance bridge using a bridge ratio of 1/500, a total resistance of 50 000 Ω in the ratio arms and a parallel configuration of the balancing arm. The bridge was excited with a sinsusoidal voltage of about 10 mV amplitude and at different frequencies. The values of R_s and C_s were then derived from the bridge readings of R_p and C_p using the well-known transformations:

$$R_s = \frac{R_p}{1 + \omega^2 C_p^2 R_p^2} \tag{7}$$

$$1/(\omega C_s) = \frac{\omega C_p R_p^2}{1 + \omega^2 C_p^2 R_p^2}. \tag{8}$$

Commercial dry (D-size, Leclanché) cells, fresh magnesium–manganese dioxide dry cells (CL size) assembled on a pilot plant and commercial sealed sintered-plate nickel–acid cells were employed in the investigation.

4. Results and discussion

Figs. 3–6 show the results obtained over a wide range of frequencies employing both the

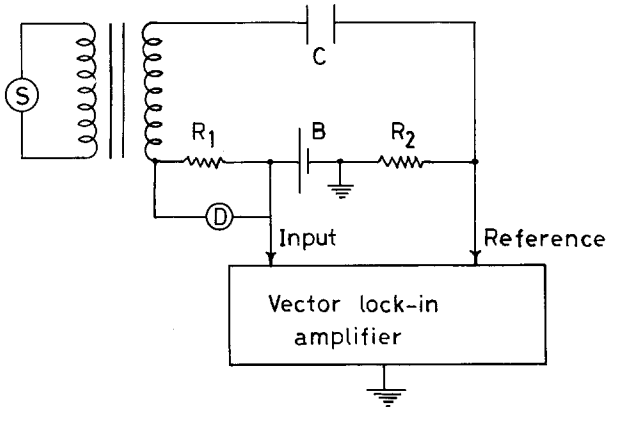

Fig. 2. Schematic diagram of the set-up for the measurement of impedance and phase-angle of a battery. S Low frequency signal generator; C Blocking capacitor (10^3 μF, 100 V); B Battery under test; R_1 Non-reactive calibrated resistance (typically 5 Ω); R_2 Non-reactive resistance of such value that the alternating voltage drop across it is about 1 V for the given alternating current in the circuit; D Digital voltmeter (input impedance 10 MΩ) with a resolution of 0·1 mV; Vector lock-in amplifier: PAR Model 129A.

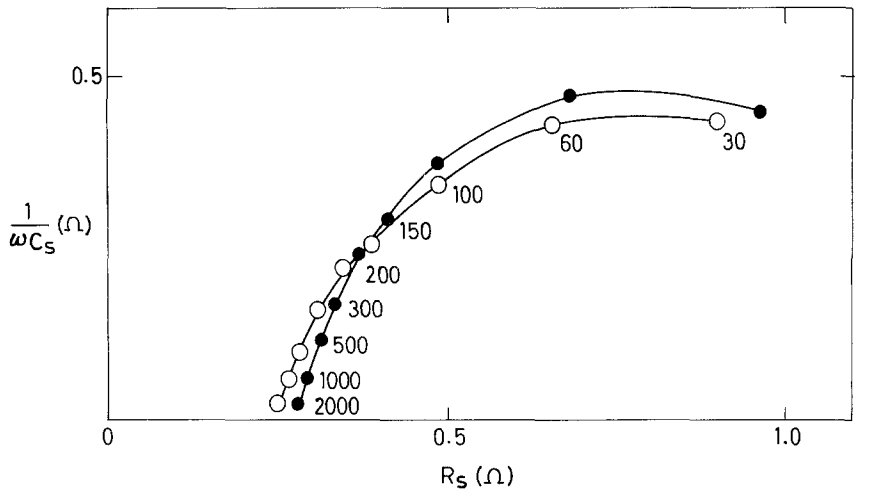

Fig. 3. Argand diagram [$1/(\omega C_S)$ versus R_S] for zinc–manganese dioxide (Leclanché) D-size cell. Points: data obtained by an impedance bridge and then using Equations 7 and 8. Circles: data obtained by measurement of impedance and phase-angle and then using Equations 3 and 4.

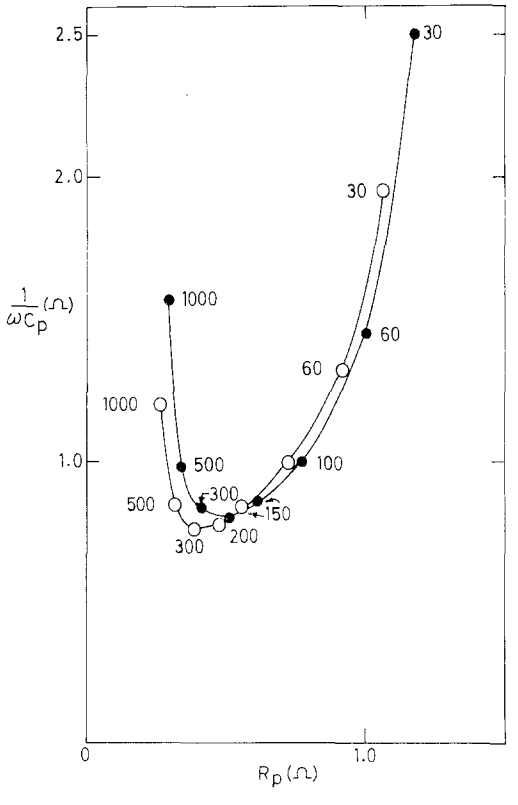

Fig. 4. Argand diagram [$1/(\omega C_p)$ versus R_p] for zinc–manganese dioxide (Leclanché) D-size cell. Points: data obtained by direct measurement with an impedance bridge. Circles: data obtained by measurement of impedance and phase-angle and then using Equation 5 and 6.

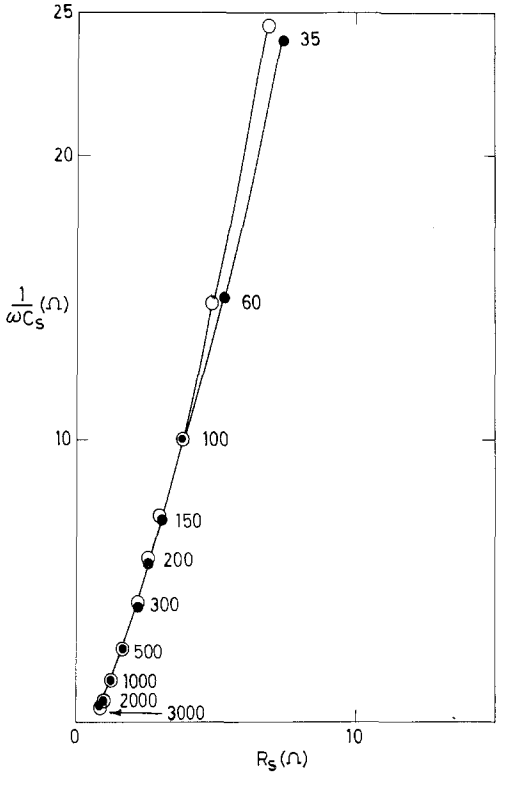

Fig. 5. Argand diagram [$1/(\omega C_S)$ versus R_S] for magnesium–manganese dioxide (CL size) dry cell. Points: data obtained by an impedance bridge and then using Equations 7 and 8. Circles: data obtained by measurement of impedance and phase-angle and then using Equations 3 and 4.

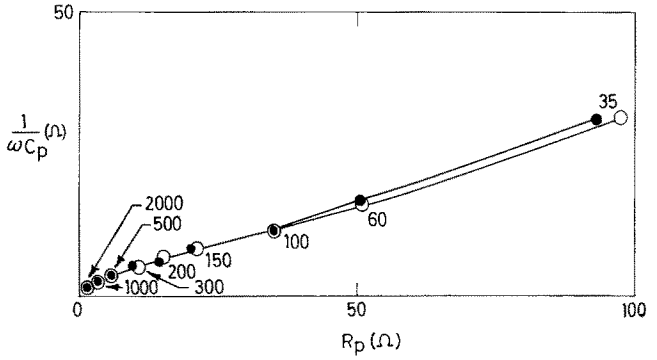

Fig. 6. Argand diagram [$1/(\omega C_p)$ versus R_p] for magnesium–manganese dioxide (CL size) dry cell. Points: data obtained by direct measurement with an impedance bridge. Circles: data obtained by measurement of impedance and phase-angle and then using Equations 5 and 6.

impedance–phase angle technique as well as the bridge technique for the dry cell systems.

It may be seen from the figures that the agreement between the two sets of measurements is quite good. The impedance–phase angle method may therefore be adopted for the determination of the effective resistance and reactance of a battery.

With lead–acid and nickel–cadmium batteries, it was found that the phase shift was of the order of 1–5° only which could not be accurately measured with the PAR lock-in amplifier used in the present work. Reliable measurements in these cases require a phasemeter of basic accuracy ± 0·1°.

The results obtained for the Leclanché system (Figs. 3 and 4) may be interpreted in terms of the conventional Randles-type equivalent circuit [3]. The trend of the curves shows that the impedance of this system is mainly under charge-transfer control in the frequency range 30–1000 Hz. The trend is similar to those reported in the literature [1].

The results obtained for the magnesium–manganese dioxide system (Figs. 5 and 6) are rather unusual since the plot of $1/(\omega C_s)$ versus R_s shows a linear behaviour with a slope of about four over a wide frequency range. These results are difficult to interpret in terms of the Randles equivalent circuit. It seems necessary to incorporate features specific to the magnesium electrode (for example, the impedance characteristics of the passive film on the magnesium electrode) into the equivalent circuit in order to explain the results with this system.

References

[1] W. J. Hamer, 'The Primary Batteries', Vol. II (eds. N. C. Cahoon and G. W. Heise) (The Electrochemical Society Series), John Wiley and Sons, London (1976).

[2] M. Sluyters-Rehbach and J. H. Sluyters, in 'Electroanalytical Chemistry' Vol. 4 (ed. A. J. Bard) Marcel Dekker Inc., New York (1970).

[3] J. McHardy, J. M. Baris and P. Stonehart, *J. Appl. Electrochem.* **6** (1976) 371.